1521-009X/47/8/919–927$35.00
Drug Metabolism and Disposition
Copyright © 2019 by The American Society for Pharmacology and Experimental Therapeutics
https://doi.org/10.1124/dmd.119.086892
Drug Metab Dispos 47:919–927, August 2019

Nitidine Chloride–Induced CYP1 Enzyme Inhibition and Alteration of Estradiol Metabolism

Xu Mao, Jian Wang, Qian Wang, Lan Yang, Yilin Li, Hao Lin, Ying Peng,[1] and Jiang Zheng[1]

Wuya College of Innovation (X.M., Q.W., L.Y., Y.L., H.L., Y.P., J.Z.) and School of Pharmaceutical Engineering (J.W.), Shenyang Pharmaceutical University, Shenyang, Liaoning, People's Republic of China; and School of Pharmacy, State Key Laboratory of Functions and Applications of Medicinal Plants, Key Laboratory of Pharmaceutics of Guizhou Province and Guizhou Medical University, Guiyang, Guizhou, People's Republic of China (J.Z.)

Received February 21, 2019; accepted May 24, 2019

ABSTRACT

The cytochrome P450 (P450) 1 family is an important phase I enzyme involved in carcinogen activation. Nitidine chloride (NC) is a pharmacologically active alkaloid with polyaromatic hydrocarbon found in the roots of *Zanthoxylum nitidum* (Roxb.) DC, a traditional medicinal herb widely used in China. We examined the inhibitory effects of NC on CYP1A1, 1B1, and 1A2. NC significantly inhibited CYP1A1- and 1B1-catalyzed ethoxyresorufin *O*-deethylation activity (IC_{50} = 0.28 ± 0.06 and 0.32 ± 0.02 μM, respectively) in a concentration-dependent manner, but only showed slight inhibition of CYP1A2 activity (IC_{50} > 50 μM). Kinetic analysis revealed that NC competitively inhibited CYP1B1 with a K_i value of 0.47 ± 0.05 μM, whereas NC caused a mixed type of inhibition on CYP1A1 with K_i and K_I values of 0.14 ± 0.04 and 0.19 ± 0.09 μM, respectively. The observed enzyme inhibition neither required NADPH nor revealed time dependency. Molecular docking manifested the generation of strong hydrogen-bonding interactions of Ser116 in CYP1A1 and Ser127 in CYP1B1 with methoxy moiety of NC. Additionally, NC-induced alteration of estradiol (E2) metabolism was also investigated in the present study. Hydroxyestradiols, including 2-hydroxyestradiol [(2-OHE2) nontoxic] and 4-hydroxyestradiol [(4-OHE2) genotoxic] generated in recombinant enzyme incubation systems and cultured MCF-7 cells were analyzed, and NC was found to preferentially inhibit the nontoxic 2-hydroxylation activity of E2 mediated by CYP1A1. In conclusion, NC was a mixed type inhibitor of CYP1A1 and a competitive inhibitor of CYP1B1. The remarkable inhibition on E2 2-hydroxylation might increase the risk of 4-OHE2–induced genotoxicity.

SIGNIFICANCE STATEMENT

CYP1 enzymes catalyze oxidative metabolism of a variety of compounds and are known to play a crucial role in the development of cancer. CYP1A1 and CYP1A2 are responsible for hydroxylation of estradiol (E2) at the C-2 position, resulting in the formation of 2-OHE2, which is proposed to be a detoxification pathway. However, CYP1B1-mediated hydroxylation of E2 at the C-4 position has been suggested to be a tumor initiator. The present study found that nitidine chloride is a mixed type inhibitor of CYP1A1 and a competitive inhibitor of CYP1B1. NC preferentially inhibited the nontoxic E2 2-hydroxylation pathway mediated by CYP1A1, which might increase the risk of 4-OHE2–induced genotoxicity and cause severe drug-drug interactions.

Introduction

Zanthoxylum nitidum (Roxb.) DC as a traditional herbal medicine is mainly distributed in Asian nations (Liao et al., 2013; Li et al., 2017). The roots of the plant have been used extensively in China for treatment of various diseases, including neuralgia, toothache, rheumatism, and swelling of the throat (Liu et al., 2017). Meanwhile, it also usually serves as a natural ingredient in commodities such as toothpaste. An abundance of alkaloids has been isolated and identified from herbal roots, and nitidine chloride (NC) (Scheme 1) is the major one of them (Arthur et al., 1959). The reported pharmacological activities of NC include antihuman immunodeficiency virus (Tan et al., 1991), anti-inflammatory (Hu et al., 2006; Wang et al., 2012), antimalarial (Gakunju et al., 1995; Bouquet et al., 2012), and antitumor agent (Iwasaki et al., 2010; Pan et al., 2011; Chen et al., 2012; Fang et al., 2014; Ou et al., 2015).

Cytochromes P450s (P450s) are heme-containing enzymes primarily responsible for oxidation or reduction of the majority of pharmaceutical agents currently in use (Foti and Dalvie, 2016). Comprised of a vast number of isoforms, this gene superfamily of proteins mostly belongs to intrahepatic enzymes (Vrba et al., 2004). The CYP1 family plays a crucial role in the phase I metabolism of endogenous and exogenous compounds such as estrogen and polyaromatic hydrocarbon and is known to be involved in the generation of carcinogens (Lo et al., 2013; Lee et al., 2016). Furthermore, CYP1 members exhibit differences in tissue distribution. Constitutive expression and production of CYP1A2 occur in human liver, whereas CYP1A1 and 1B1 are mainly localized in extrahepatic tissues (Lo et al., 2013).

Estradiol (E2) (Scheme 1) is a natural estrogen with many physiologic effects (Lozan et al., 2017). Oxidation of E2 to 2-hydroxyestradiol (2-OHE2) and 4-hydroxyestradiol (4-OHE2) mediated by CYP1A1, 1B1, and 1A2 has been suggested to be associated with detoxification and

[1]J.Z. and Y.P. contributed equally to this work.

The authors declare that there are no conflicts of interest.

This work was supported in part by the National Natural Science Foundation of China [Grants 81830104, 81430086, 81773813, and U1812403].

https://doi.org/10.1124/dmd.119.086892.

ABBREVIATIONS: E2, estradiol; EE2, ethinyloestradiol; ERF, ethoxyresorufin; EROD, ethoxyresorufin *O*-deethylation; IS, internal standard; LC-MS/MS, liquid chromatography–tandem mass spectrometry; *m/z*, mass-to-charge ratio; NC, nitidine chloride; α-NF, α-naphthoflavone; 2-OHE2, 2-hydroxyestradiol; 4-OHE2, 4-hydroxyestradiol; P450, cytochrome P450.

Downloaded from dmd.aspetjournals.org at ASPET Journals on April 16, 2024

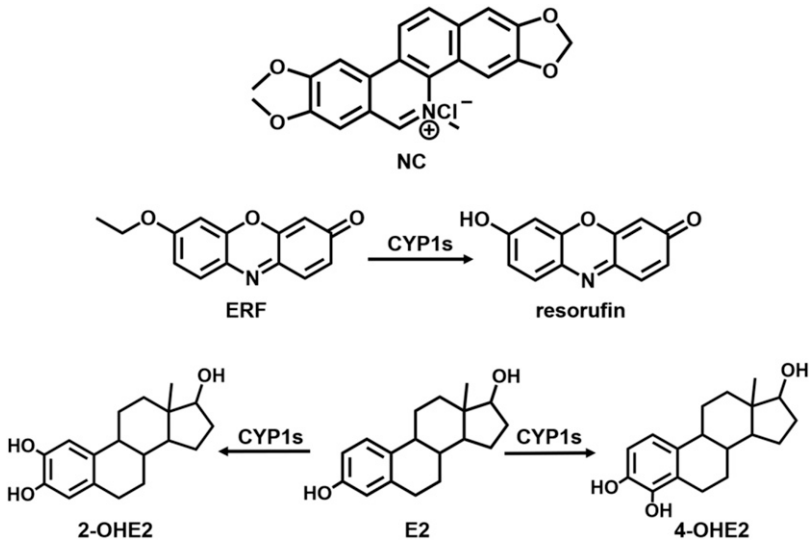

Scheme 1. Chemical structures of NC (A), ERF (B), and E2 (C).

tumorigenesis, respectively (Lakhani et al., 2003; Lee et al., 2003). Many CYP1 inhibitors have been demonstrated to share several structural motifs that are planar with two or more hydrophobic aromatic rings (Zanger and Schwab, 2013; Lee et al., 2016). For example, sanguinarine is identified to be a noncompetitive inhibitor of CYP1A1 and a competitive inhibitor of CYP1A2 (Vrba et al., 2004). Berberine potently inhibits CYP1B1 activity, whereas CYP1A2 exhibits resistance to the inhibition (Lo et al., 2015). This led us to speculate that NC may induce CYP1 enzyme inhibition.

With the rapidly growing global interest in the use of natural products as dietary supplements and medical remedies, rigorous interdisciplinary studies on the efficacy, potential toxicity, and health benefits of these botanicals have become increasingly and considerably significant. In the present study, we investigated the interactions of NC with human recombinant CYP1 enzymes and explored the alteration of E2 metabolism mediated by NC.

Materials and Methods

Chemicals and Materials. Nitidine chloride was used in the study with purity >98%, which was acquired from Chengdu Push Bio-Technology Co., Ltd. (Chengdu, China). Human recombinant CYP1A2 and CYP1B1 were obtained from BD Gentest (Woburn, MA). Human recombinant CYP1A1 was purchased from Cypex (Dundee, UK). Ethoxyresorufin (ERF), resorufin, E2, ethinyloestradiol (EE2), dansyl chloride, α-naphthoflavone (α-NF), and propranolol were supplied by Aladdin Industrial Corporation (Shanghai, China). NADPH was acquired from Sigma-Aldrich (St. Louis, MO). 2-OHE2 and 4-OHE2 were purchased from Toronto Research Chemicals Inc. (Toronto, Canada).

Determination of IC_{50} Values of NC-Mediated Inhibition of CYP1A1, 1B1, and 1A2. Ethoxyresorufin *O*-deethylation (EROD) assays (Scheme 1) were performed with CYP1 enzymes to measure enzyme inhibition, according to a published method (Henderson et al., 2000). Briefly, CYP1A1, CYP1B1, or CYP1A2 (5.0 nM) was incubated with ERF (2.0 μM) in 200 μl of 100 mM potassium phosphate buffer (pH 7.4) containing NC (0–100 μM) and $MgCl_2$ (3.2 mM). The incubations were started by adding NADPH (1.0 mM). In addition, α-NF, a known selective inhibitor of CYP1 enzymes (Shimada, 2017), was incubated with ERF as described previously to ensure the involvement of CYP1 enzymes in EROD metabolism. After 10-minute incubation at 37°C, the reaction mixtures were quenched with 200 μl ice-cold acetonitrile consisting of 50 ng/ml propranolol [internal standard (IS)], and then centrifuged at 19,000*g* for 10 minutes to remove protein. The supernatants were analyzed by the liquid chromatography–tandem mass spectrometry (LC-MS/MS) system as will be described subsequently. The formation of de-ethylation metabolite was linear for the first 10 minutes, and the concentrations of NC and α-NF required for 50% inhibition of catalytic activity (IC_{50} values) were calculated by curve fitting.

Determination of Kinetic Values for NC-Induced Inhibition of CYP1A1 and CYP1B1. The kinetic values for NC-induced inhibition of CYP1 enzymes were determined by EROD assays. ERF (0.05–5 μM) was mixed with CYP1A1 or CYP1B1 (5.0 nM) in the presence of NC at concentrations of 0, 0.1, 0.5, or 2.5 μM. The same procedure was carried out for reaction initiation, reaction termination, and sample preparation as described previously. EROD activity was measured by LC-MS/MS–based monitoring of resorufin formation as follows. Enzyme activities were assessed by an established resorufin standard curve. Specifically, calibration standards were obtained by serially diluting resorufin stock solutions with PBS to final concentrations of 0.5, 1.0, 2.0, 5.0, 25, 100, and 500 nM, followed by adding an equal volume of ice-cold acetonitrile with 50 ng/ml propranolol (IS). Seven-point calibration curves were estimated by the plot of the response ratios of analytes to the IS (resorufin) against the resorufin concentrations, and the linearity was verified by applying the $1/x$-weighted linear regression method.

Determination of Time- and NADPH-Dependent Inhibitory Effects of NC on CYP1A1 and CYP1B1. Recombinant CYP1A1 or CYP1B1 (50 nM), NC (0 and 100 μM), and $MgCl_2$ (3.2 mM) were mixed in 120 μl PBS, followed by addition of NADPH (1.0 mM) for the initiation of the reaction. After incubation at 37°C for 0, 5, 15, and 30 minutes, aliquots (20 μl) were withdrawn and transferred to secondary incubation mixtures containing ERF (2.0 μM), $MgCl_2$ (2.0 mM), and NADPH (0.5 mM). The resulting mixture was incubated at 37°C for 10 minutes. In a separate study, similar microsomal incubation without NADPH was carried out to determine the effect of NADPH on enzyme inhibition. The reactions were terminated by adding an equal volume of ice-cold acetonitrile that contained propranolol as the IS. After deproteination by centrifuging, the resulting supernatants were submitted to LC-MS/MS analysis for assessment of residual catalytic activity.

Determination of IC_{50} Values of NC-Induced Inhibition of 2- and 4-Hydroxylation of E2 Mediated by CYP1 Enzymes. The incubation mixtures were composed of E2 (20 μM), NC (0–100 μM), and $MgCl_2$ (3.2 mM) fortified

TABLE 1

NC- and α-NF–induced inhibition of EROD activity of CYP1A1, CYP1B1, and CYP1A2

Data represent the mean ± S.D. (n = 3).

Inhibitor	IC_{50}		
	CYP1A1	CYP1B1	CYP1A2
	μM	μM	μM
NC	0.28 ± 0.06	0.32 ± 0.02	>50
α-NF	0.12 ± 0.03	0.06 ± 0.01	0.51 ± 0.12

Downloaded from dmd.aspetjournals.org at ASPET Journals on April 16, 2024

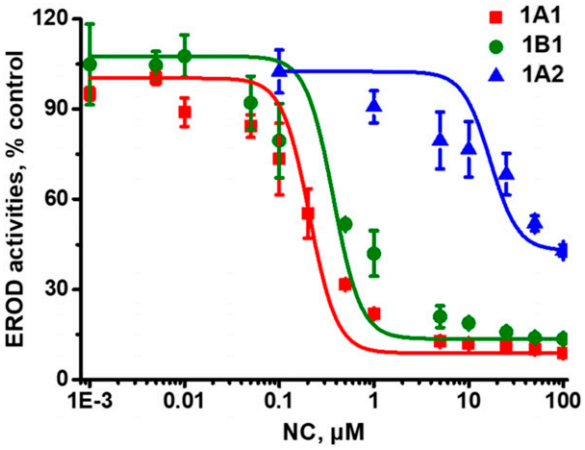

Fig. 1. NC-Induced inhibition of EROD activity catalyzed by CYP1 enzymes. CYP1A1, CYP1B1, or CYP1A2 (5 nM) was incubated with ERF (2.0 μM) and NC (0–100 μM) at 37°C for 10 minutes, followed by assessment of remaining enzyme activity. Data represent the mean ± S.D. (n = 3).

with CYP1A1, CYP1B1, or CYP1A2 (10 nM) in 100 μl of potassium phosphate buffer (100 mM, pH 7.4) containing 0.1% ascorbic acid. The enzymatic reactions were initiated by addition of NADPH (1.0 mM), followed by incubation at 37°C for 10 minutes. Reactions were stopped by mixing 500 μl of ethyl acetate with EE2 (IS, 25 nM). After vortexing for 30 seconds, the organic layer was collected and concentrated under a stream of nitrogen gas, and then the residues were dissolved in 100 μl of sodium bicarbonate buffer (0.1 M, pH 9.0) and 100 μl dansyl chloride (1.0 mg/ml in acetone). The solution was incubated at 60°C for 20 minutes. The resulting samples were cooled on ice and centrifuged at 19,000g for 10 minutes. The supernatants were injected into the LC-MS/MS system for analysis as subsequently described.

Determination of Kinetic Parameters for NC-Induced Inhibition of E2 Hydroxylation Mediated by CYP1A1. The incubations containing CYP1A1 (10 nM) and E2 (0.5–80 μM) were performed with NC at concentrations of 0, 0.05, 0.1, 0.2, or 0.5 μM and NADPH (1.0 mM) at 37°C for 10 minutes. The resulting incubation mixtures and metabolite standards (2-OHE2 and 4-OHE2) were extracted and derivatized following the same procedure as previously described. After derivatization, all samples were analyzed by LC-MS/MS.

Cell Culture. MCF-7 cells were generously provided by Dr. F.J. Zhang (Shenyang Pharmaceutical University). Cells were cultured in Dulbecco's modified Eagle's medium (HyClone; GE Healthcare Life Sciences, China) fortified with 10% FBS (Gibco, Australia) and 1% penicillin-streptomycin solution (HyClone; GE Healthcare Life Sciences) at 37°C in a 5% CO_2 environment.

Evaluation of NC-Induced Inhibition of 2- and 4-Hydroxylation of E2 Mediated by CYP1 Enzymes in MCF-7 Cells. MCF-7 cells were seeded on 24-well plates at a density of 1.2 × 10^5 cells per well. Following 24 hours of stabilization, cells were treated with Dulbecco's modified Eagle's medium containing NC (5.0, 10, and 20 μM). DMSO (0.4% v/v) was used as a negative control. After incubating for 1 hour, culture media were removed. The cells were washed once with PBS, followed by addition of E2 (1.0 μM) and 24-hour incubation. Cell media (1.0 ml) were then collected and extracted with ethyl acetate (2 × 2 ml) containing EE2 (IS, 5.0 nM) and 0.1% ascorbic acid. The organic layers were combined and dried under a gentle flow of nitrogen. The residues were derivatized as described previously, and the resultant samples were submitted to LC-MS/MS for analysis.

Simulation of Binding of NC with CYP1 Enzymes by Computer Modeling and Docking. The LibDock module with the LibDockScore scoring function of Discovery Studio version 3.0 was employed to perform the computer modeling of NC. The docking of NC to putative active sites of three CYP1 enzymes was generated using crystallographic structures of CYP1A2 (Protein Data Bank Identification: 2HI4), CYP1A1 (Protein Data Bank Identification: 4I8V), and CYP1B1 (Protein Data Bank Identification: 3 PM0). During the docking process, the top 10 conformations were saved for each ligand based on the dock score value after energy minimization using the smart minimize method through the LibDock program. Finally, docking models of NC with CYP1 members were displayed by the PyMOL software program (http://www.pymol.org).

LC-MS/MS Analysis Method. NC-mediated inhibition of EROD and E2 hydroxylation activity catalyzed by CYP1 enzymes was assessed by monitoring the generation of de-ethylation and hydroxylation metabolites, respectively. The products were analyzed on a 5500 triple quadrupole mass spectrometer from AB Sciex (Applied Biosystems, Foster City, CA) interfaced online with an Agilent 1260 Series HPLC (Agilent Technologies, Santa Clara, CA). Chromatographic separation was achieved on an analytical Promosil C_{18} column (100 × 4.6 mm, 5.0 μm; Agela Technologies, Inc., Tianjin, China) at the temperature of 25°C. Gradient elution was performed for resorufin with a flow rate of 0.8 ml/min, including mobile phase A (acetonitrile with 0.1% formic acid) and mobile phase B (water with 0.1% formic acid). The high-performance liquid chromatography gradient was set as follows: 10% A at 0–2.0 minutes; 10%–40% A at 2.0–2.5 minutes; 40%–95% A at 2.5–6.0 minutes; 95% A at 6.0–9.0 minutes; 95%–10% A at 9.0–9.5 minutes; and 10% A at 9.5–11.0 minutes. Isocratic elution was conducted for derivatized 2-OHE2 and 4-OHE2 with 88% (A) at a 1.0 ml/min flow rate. The injection volume was 5.0 μl. Quantification was conducted with an electrospray ionization source in positive mode. Multiple reactions monitoring scanning was used for targeted analysis with the ion transition (corresponding to collision energy and declustering potential) mass-to-charge ratio (m/z) 214.0 →186.0 for metabolite resorufin (35, 70), m/z 755.0 →521.0 for derivatized metabolites 2-OHE2 and 4-OHE2 (44, 50), m/z 260.3 →116.3 for IS propranolol (44, 77), and m/z 530.0 →171.0 for derivatized IS EE2 (35, 30), respectively. All operations and data analysis

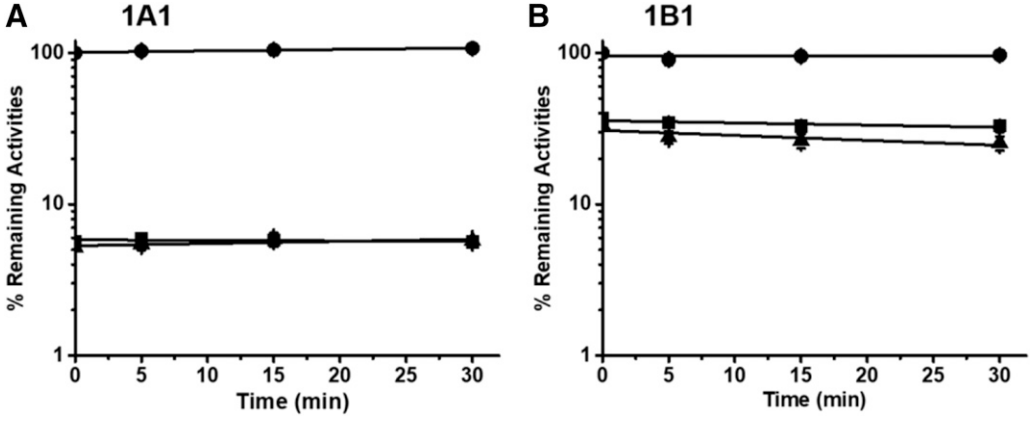

Fig. 2. Time- and NADPH-dependent inhibition of CYP1A1 (A) and CYP1B1 (B) by NC. CYP1A1 or CYP1B1 (50 nM) was incubated with vehicle (●) and NC (100 μM) in the presence (▲) or absence (■) of NADPH at 37°C for 0, 5, 15, and 30 minutes. Aliquots of the incubation mixtures were transferred to secondary incubation mixtures for determination of residual enzymatic activity.

Downloaded from dmd.aspetjournals.org at ASPET Journals on April 16, 2024

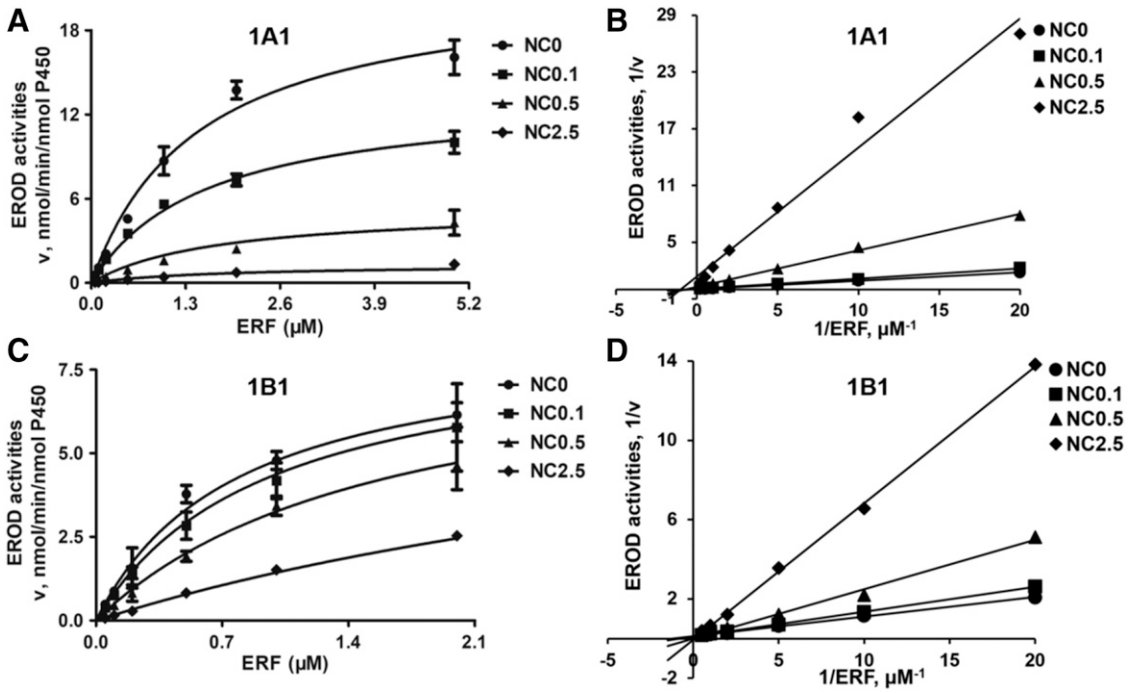

Fig. 3. Kinetic analysis of NC-induced inhibition of EROD activity in a human recombinant CYP1A1 or CYP1B1 system. (A and C) show the velocity (v) vs. ERF concentration (S) plots of activity in the presence of NC at various concentrations as indicated. (B and D) show the Lineweaver-Burk plots for NC-induced inhibition of EROD activity mediated by CYP1A1 and CYP1B1. Data represent the mean ± S.D. (n = 3).

were processed by the Analyst software program (version 1.6.3; Applied Biosystems).

Data Analysis and Statistics. To evaluate NC-induced inhibition of CYP1A1 and 1B1 and alteration of E2 metabolism, kinetic analyses were conducted following the Michaelis-Menten kinetic property. Velocity-substrate concentration (*V-S*) curves were fitted by no-weighting nonlinear least-squares regression, according to the Michaelis-Menten equation in the GraphPad Prism 5 software program (GraphPad Co. Ltd., San Diego, CA). The data were expressed as the mean ± S.D. of three independent experiments. For different types of inhibition, the kinetic values (K_I and K_i) were calculated as follows:

$$\text{Competitive inhibition: } v = \frac{V_{max} \cdot S}{S + K_m[1 + (I/K_i)]}$$

$$\text{Noncompetitive inhibition: } v = \frac{V_{max} \cdot S}{[S + K_m][1 + (I/K_i)]}$$

$$\text{Mixed type of inhibition: } v = \frac{V_{max} \cdot S}{S[1 + (I/K_I)] + K_m[1 + (I/K_i)]}$$

where I and V_{max} are the NC concentration and maximal velocity, respectively; K_m is the substrate concentration at one-half the V_{max} value of the reaction; and K_i and K_I are the inhibition constants for the binding of an inhibitor to the enzyme and enzyme-substrate complex, respectively.

Results

NC-Induced Inhibition of CYP1 Enzymes. EROD assays with recombinant enzymes were conducted to investigate NC-induced inhibitory effects on CYP1 enzymes. Among the three isozymes, NC was found to cause potent inhibition of CYP1A1 and CYP1B1 activities in a concentration-dependent manner with IC_{50} values of 0.28 ± 0.06 and 0.32 ± 0.02 μM, respectively (Table 1). However, the inhibitory efficiency of NC on CYP1A2 ($IC_{50} > 50$ μM) was considerably lower than that with CYP1A1 or CYP1B1 (Fig. 1). The IC_{50} values obtained from inhibition tests by α-NF are also listed in Table 1. These data indicate that NC selectively inhibited CYP1A1 and CYP1B1 activities, especially CYP1A1 activity.

Time- and NADPH-Dependent Inhibition of NC on CYP1A1 and CYP1B1. We initially probed different preincubation times on the inhibitory effects of CYP1A1 and CYP1B1 activities mediated by NC. As shown in Fig. 2, NC showed no time-dependent inhibition on CYP1A1 and 1B1. We also tested whether the presence of NADPH is required for enzymatic inactivation induced by NC. No significant difference in CYP1A1 and CYP1B1 activities was found after 30-minute microsomal incubation with or without NADPH. These results suggest that NC is a reversible inhibitor of CYP1A1 and CYP1B1.

Kinetic Analysis of NC-Induced Inhibition on CYP1A1 and CYP1B1. According to the aforementioned IC_{50} results, CYP1A2-mediated EROD activity was hardly inhibited by NC. Thus, kinetic studies were carried out to further evaluate NC-induced inhibition on CYP1A1 and CYP1B1. Nonlinear regression analysis for competitive or mixed inhibition using GraphPad Prism 5 was used to determine the apparent K_i values and the mode of inhibition. The correlation coefficients (r) were 0.968–0.995. CYP1A1 catalyzed EROD activity with V_{max} and K_m values of 21.0 ± 2.3 nmol/min per nanomoles P450 and 1.30 ± 0.36 μM, respectively. CYP1B1 catalyzed EROD activity with V_{max} and K_m values of 5.71 ± 0.39 nmol/min per nanomoles P450

TABLE 2

Kinetic parameters of NC-induced inhibition of EROD activity of CYP1A1, CYP1B1, and CYP1A2

Data represent the mean ± S.D. (n = 3).

CYP1 Enzyme	EROD		
	Type of Inhibition	K_i	K_I
		μM	μM
1A1	Mixed	0.14 ± 0.04	0.19 ± 0.09
1B1	Competitive	0.47 ± 0.05	

Downloaded from dmd.aspetjournals.org at ASPET Journals on April 16, 2024

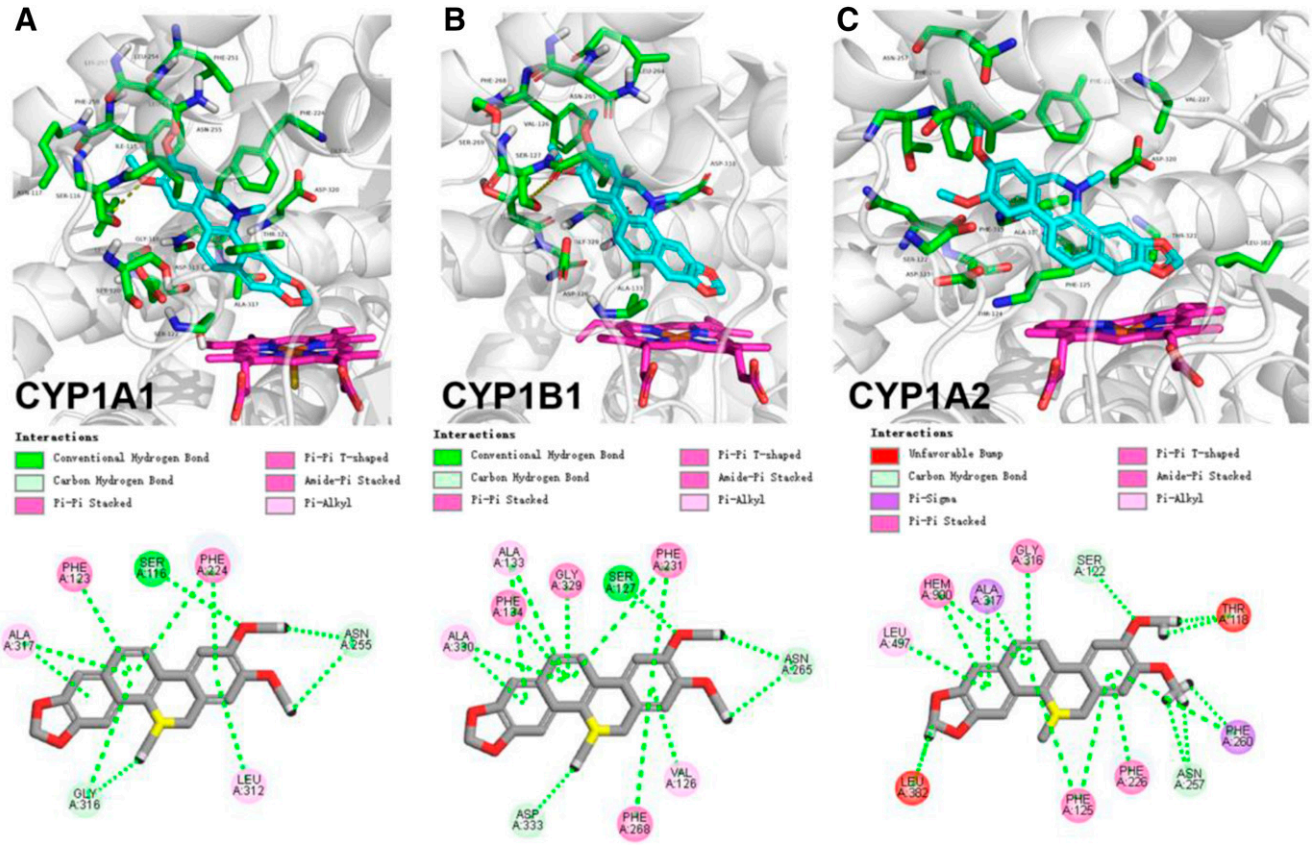

Fig. 4. Three-dimensional structural docking of NC with CYP1A1 (A), CYP1B1 (B), and CYP1A2 (C). The nitrogen and oxygen atoms are shown in dark blue and red, respectively. The heme prosthetic group of P450 enzymes is shown in magenta with iron in dark red. The hydrogen bond formation between NC and the amino acid residues of apoprotein of CYP1 enzymes is shown by yellow dashed lines.

and 0.31 ± 0.03 μM, respectively. NC competitively inhibited CYP1B1 activity with a K_i value of 0.47 ± 0.05 μM. However, NC produced a mixed type of inhibition of CYP1A1 with K_i and K_I values of 0.14 ± 0.04 and 0.19 ± 0.09 μM, respectively (Fig. 3; Table 2). The kinetic value (K_i) of CYP1B1 inhibition by NC was higher than that of CYP1A1 (K_i and K_I), which is in accordance with the IC_{50} results obtained.

Molecular Docking of NC with CYP1A1, 1A2, and 1B1. To assist the explanation for the observed inhibition of CYP1A1 and 1B1, computer modeling of the binding of NC to CYP1 enzymes was performed to compare NC affinity with the three CYP1 enzymes and to define the interactions with the crucial amino acid residue(s). LibDock was used to perform the interplay of NC with CYP1 enzymes (Fig. 4). The dockings of NC to the active sites of CYP1 enzymes showed LibDockScore values in the order of CYP1A1 (153.191) > CYP1B1 (151.352) > CYP1A2 (120.382). The binding of NC to CYP1A1 displayed a higher score with a lower IC_{50} value in activity inhibition (Table 1). The methylenedioxy ring of NC lay closely to the heme moiety of the three CYP1 members. Ser127 of CYP1B1 and Ser116 of CYP1A1 were found to interact with one of the methoxy moieties of NC via hydrogen bonds, respectively. However, no hydrogen bond

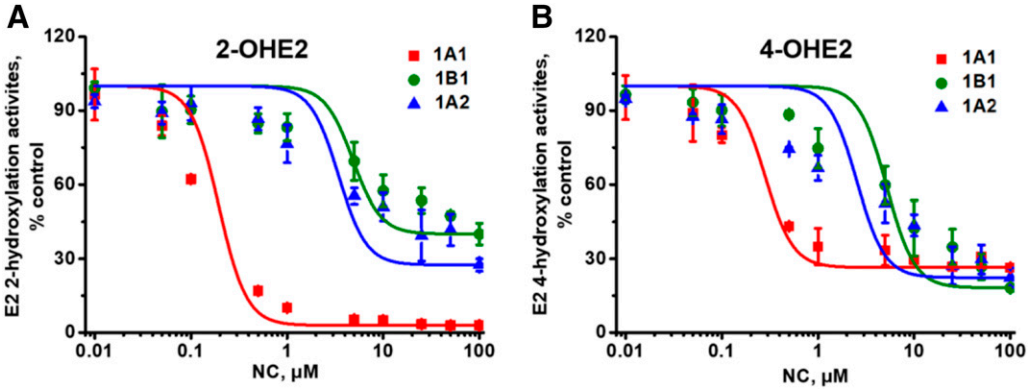

Fig. 5. NC-induced inhibition of E2 2-hydroxylation (A) and 4-hydroxylation (B) activities catalyzed by CYP1 enzymes. CYP1A1, CYP1B1, or CYP1A2 (10 nM) was incubated with E2 (20 μM) and NC (0–100 μM), followed by assessment of remaining enzyme activity. Data represent the mean ± S.D. (n = 3).

Downloaded from dmd.aspetjournals.org at ASPET Journals on April 16, 2024

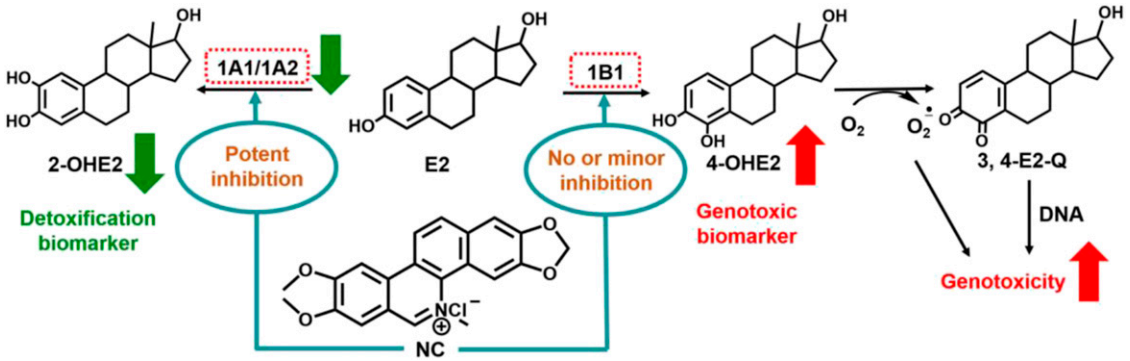

Scheme 2. Proposed effect of NC on E2 chemical carcinogenesis. CYP1A1 and 1A2 primarily catalyze the formation of 2-OHE2 (detoxification biomarker). CYP1B1 primarily catalyzes the formation of 4-OHE2 (genotoxic biomarker), which is further oxidized to genotoxic estradiol-3,4-quinone (3,4-E2-Q). NC has been reportedly demonstrated to markedly decrease 2-hydroxylation and relatively increase 4-hydroxylation metabolism of E2, as shown by the green and red arrows.

formation was found between the methoxy moieties of NC and CYP1A2. Instead, two unfavorable interaction bonds were observed in CYP1A2. Other chemical interactions, including π-π, π-alkyl, etc., are presented in Fig. 4. There was no significant difference between CYP1 isozymes in forming hydrophobic interactions with NC. The docking results suggest that Ser127 of CYP1B1 and Ser116 of CYP1A1 might be of significance in NC-induced enzyme inhibition.

NC-Induced Inhibition of 2- and 4-Hydroxylation of E2 Mediated by CYP1 Enzymes. Coincubation studies were performed to determine the inhibitory effects of NC on CYP1 enzyme–mediated E2 hydroxylation. NC showed prominent inhibition on CYP1A1-catalyzed 2- and 4-hydroxylation of E2 with IC_{50} values of 0.16 ± 0.004 and 0.25 ± 0.04 μM, respectively, which were significantly lower than the values for CYP1A2 (IC_{50} = 13.2 ± 5.56 and 5.35 ± 0.62 μM) and CYP1B1 (IC_{50} = 35.0 ± 6.44 and 8.27 ± 2.40 μM) (Fig. 5; Table 3). Furthermore, the IC_{50} value for the inhibition of 2-hydroxylation activity of CYP1A1 was about 60% of that for 4-hydroxylation, revealing that NC preferentially inhibited CYP1A1-mediated E2 2-hydroxylation activity.

Kinetic Parameters for NC-Induced Inhibition of E2 Hydroxylation Mediated by CYP1A1. Due to the strong inhibition of CYP1A1-mediated 2- and 4-hydroxylation of E2 by NC, kinetic analyses were conducted with various concentrations of NC in the CYP1A1 system to characterize the type of reversible inhibition. The plots of the velocity versus substrate concentrations in CYP1A1-catalyzed 2- and 4-hydroxylation of E2 showed hyperbolicity (Fig. 6, A and C). The K_m and V_{max} values for 2-hydroxylation of E2 by CYP1A1, 1B1, and 1A2 were 3.38 ± 0.69, 2.26 ± 0.30, and 23.7 ± 4.06 μM, and 6.91 ± 0.33, 0.45 ± 0.04, and 50.6 ± 4.93 nmol/min per nanomoles P450, respectively. The K_m and V_{max} values for 4-hydroxylation of E2 by CYP1A1, 1B1, and 1A2 were 28.9 ± 11.5, 0.87 ± 0.16, and 24.8 ± 4.78 μM, and 0.22 ± 0.04, 1.21 ± 0.12, and 0.97 ± 0.14 nmol/min per nanomoles P450, respectively (Table 3). The catalytic efficiency (V_{max}/K_m) of CYP1 enzyme–mediated 2- and 4-hydroxylation of E2 were 2.04 and 0.008 ml/min per nanomoles P450 (CYP1A1), 0.20 and 1.39 ml/min per nanomoles P450 (CYP1B1), and 2.14 and 0.039 ml/min per nanomoles P450 (CYP1A2), respectively (Table 3). The calculated activity ratio (2-/4-hydroxylation) of CYP1A1, 1B1, and 1A2 were 255, 0.14, and 55, respectively, indicating that CYP1A1 and 1A2 primarily catalyzed the formation of 2-OHE2, and CYP1B1 primarily catalyzed the formation of 4-OHE2 (Scheme 2; Table 3). Lineweaver-Burk plots showed that NC-induced inhibition of E2 2-hydroxylation activity mediated by CYP1A1 was best fit to a mixed type of inhibition with K_i and K_I values of 0.052 ± 0.007 and 0.210 ± 0.016 μM (Fig. 6B; Table 4). E2 4-hydroxylation activity inhibition by NC was fit well to a competitive inhibition model with a K_i value of 0.26 ± 0.03 μM (Fig. 6D; Table 4).

Effects of NC on the Formation of E2-Hydroxylation Metabolites Mediated by CYP1 Enzymes in MCF-7 Cells. As further investigation, the potential inhibitory effects of NC on CYP1A1 and 1B1 were evaluated in MCF-7 cells. As shown in Fig. 7, both 2- and 4-OHE2 were detected in cell media after E2 (1.0 μM) treatment with or without NC. The relative amounts of 2- and 4-OHE2 generated in vehicle- and NC-treated groups were estimated. As expected, NC elicited inhibitory effects on 2- and 4-hydroxylation of E2 in a concentration-dependent manner. Additionally, significantly decreased levels of 2-OHE2 were found after cells were treated with NC at concentrations of 10 μM ($P < 0.05$) or 20 μM ($P < 0.01$). The results suggest that NC

TABLE 3

NC-Induced inhibition of E2 hydroxylation activity of CYP1A1, CYP1B1, and CYP1A2

Data represent the mean ± S.D. (n = 3).

CYP1 Enzyme	E2 Hydroxylation Site	K_m	V_{max}	V_{max}/K_m	Activity Ratio (2-/4-)	IC_{50}	IC_{50} Ratio (2-/4-)
		μM	*nmol/min per nanomoles P450*	*ml/min per nanomoles P450*		*μM*	
1A1	2-OHE2	3.38 ± 0.69	6.91 ± 0.33	2.04	255	0.16 ± 0.004	0.64
	4-OHE2	28.9 ± 11.5	0.22 ± 0.04	0.008		0.25 ± 0.04	
1B1	2-OHE2	2.26 ± 0.30	0.45 ± 0.04	0.20	0.14	35.0 ± 6.44	4.23
	4-OHE2	0.87 ± 0.16	1.21 ± 0.12	1.39		8.27 ± 2.40	
1A2	2-OHE2	23.7 ± 4.06	50.6 ± 4.93	2.14	55	13.2 ± 5.56	2.47
	4-OHE2	24.8 ± 4.78	0.97 ± 0.14	0.04		5.35 ± 0.62	

2-/4-, 2-/4-hydroxylation.

Downloaded from dmd.aspetjournals.org at ASPET Journals on April 16, 2024

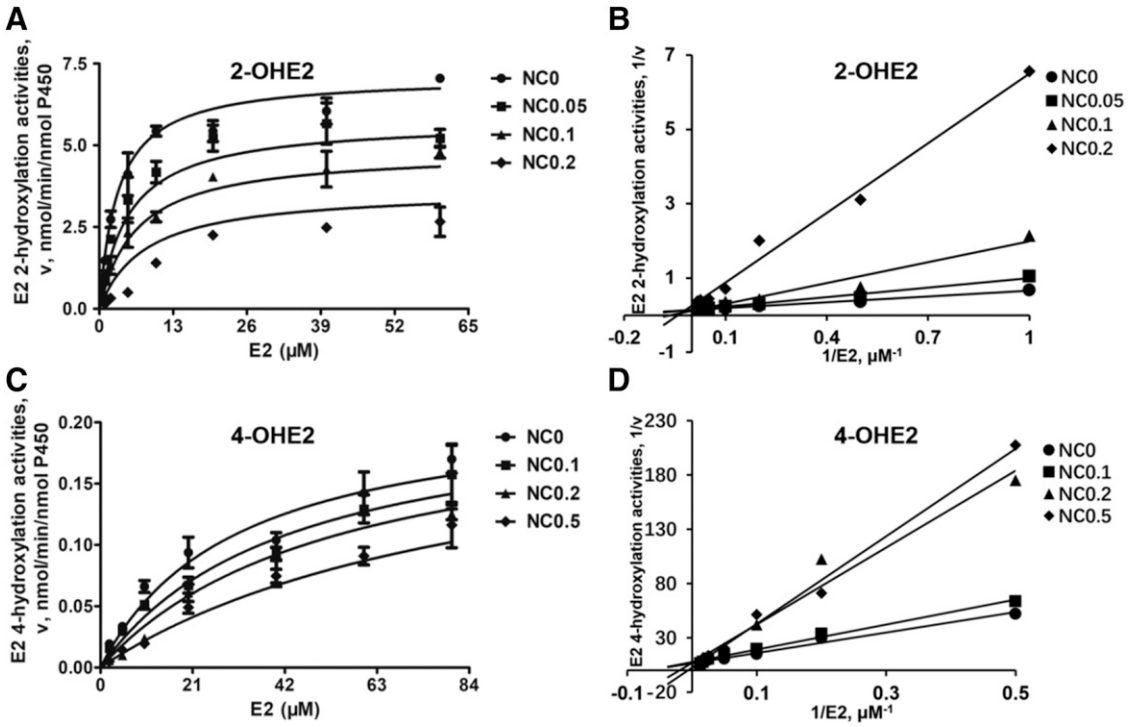

Fig. 6. Kinetic analysis of NC-induced inhibition of E2 hydroxylation activity in a human recombinant CYP1A1 system. (A and C) show the velocity (v) vs. E2 concentration (S) plots of activity in the presence of NC at various concentrations as indicated. (B and D) show the Lineweaver-Burk plots for NC-induced inhibition of E2 hydroxylation activity mediated by CYP1A1. Data represent the mean ± S.D. (n = 3).

had a stronger inhibition effect on the formation of nontoxic 2-OHE2 in MCF-7 cells.

Discussion

Botanical dietary supplements consisting of a variety of chemopreventive constituents with many pharmacological activities are popularly used as natural alternatives to medicines. However, drug-drug interactions are frequently caused by some natural product–mediated P450 enzyme inhibition, possibly resulting in severe adverse effects (Danton et al., 2013). P450 inhibition can be classified into reversible and irreversible inhibition (VandenBrink and Isoherranen, 2010). P450s are important phase I enzymes responsible for various biotransformations of endogenous substrates and xenobiotics, not only existing in intrahepatic tissues but also extensively distributed across extrahepatic tissues (Vrba et al., 2004; Liu et al., 2017). Thus, safe consumption of such natural products is becoming a public concern. NC is the major component in *Zanthoxylum nitidum* (Roxb.) DC widely used in traditional Chinese medicine. Our previous research demonstrated that NC shows no remarkable time-dependent inhibition on other major P450 enzymes in liver except for CYP2D6 (Mao et al., 2018). Carbene intermediate produced in the metabolic pathway of the methylenedioxyphenyl group of NC might lead to the quasi-irreversible inactivation of CYP2D6. In the present study, we examined the inhibitory effects of NC on three CYP1 isozymes that are considered to be linked with the generation of carcinogens. The majority of CYP1 inhibitors contain two or more fused aromatics, exhibiting molecular planarity. Heterocyclic rings and nitrogen frequently occur in such inhibitors as part of the ring system and/or in a substituent group (Zanger and Schwab, 2013; Lee et al., 2016). NC is such a polyaromatic hydrocarbon compound containing a nitrogen heterocycle. Our findings revealed that NC efficiently inhibited EROD activities mediated by CYP1A1 and CYP1B1 in a concentration-dependent manner with IC_{50} values of 0.28 and 0.32 μM, respectively, but CYP1A2 was resistant to the inhibition by NC (Fig. 1; Table 1). However, time- and NADPH-dependent inhibition of CYP1 enzymes by NC was not observed under the present conditions (Fig. 2), indicating that NC is a reversible inhibitor of CYP1A1 and 1B1. Further kinetic studies clearly demonstrated that NC exhibited competitive inhibition of CYP1B1 with a K_i value of 0.47 μM, suggesting that NC bound to the same pocket of CYP1B1 enzyme as that for ERF (Fig. 3; Table 2). NC showed the a mixed type of inhibition for CYP1A1 with lower K_i and K_I values of 0.14 and

TABLE 4

Kinetic parameters of NC-induced inhibition of E2 hydroxylation activity of CYP1A1, CYP1B1, and CYP1A2

Data represent the mean ± S.D. (n = *3).*

CYP1 Enzyme	E2 Hydroxylation			
	E2 Hydroxylation Site	Type of Inhibition	K_i	K_I
			μM	μM
1A1	2-OHE2	Mixed	0.052 ± 0.007	0.210 ± 0.016
	4-OHE2	Competitive	0.26 ± 0.03	

Downloaded from dmd.aspetjournals.org at ASPET Journals on April 16, 2024

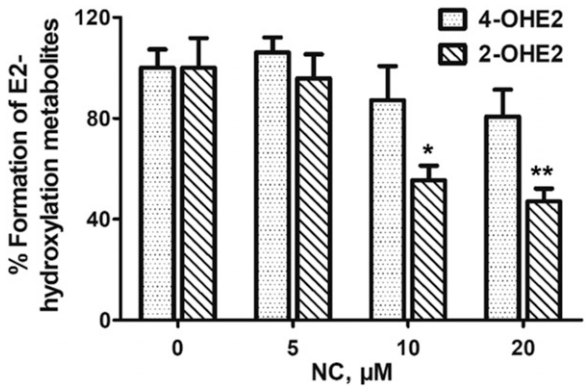

Fig. 7. Effect of NC on the formation of E2-hydroxylation metabolites (2- and 4-OHE2) in MCF-7 cells. Data represent the mean ± S.D. (n = 3).

0.19 μM, respectively, which suggests that NC does not only share the identical binding pocket with the probe substrate (ERF) but can also bind to a different pocket of the CYP1A1 enzyme. This observation indicates that NC demonstrated more significant inhibitory effects for CYP1A1 than for CYP1B1. In addition, molecular modeling of NC with CYP1 enzymes was conducted to help clarify the NC-induced difference in inhibition of the three enzymes. Hydrogen-bonding and π-π interactions were proposed to play a critical role in the binding of alkoxy derivatives of heterocyclic compounds to CYP1 enzymes (Lo et al., 2013). NC was found to interact with amino acid residue Ser127 of CYP1B1 or Ser116 of CYP1A1 via hydrogen-bonding interactions, respectively, but no such hydrogen bond was generated in CYP1A2 (Fig. 4). The LibDock-Score results also showed that the affinities of NC with CYP1A1 and 1B1 were higher than that of CYP1A2. Based on the docking score and molecular interactions with active site residues, the hydrogen bonds of CYP1A1 and CYP1B1 formed with NC might increase the inhibitory susceptibility of the two enzymes.

E2 is one of the major estrogens in women and has been the standard treatment option for postmenopausal symptom relief for decades (Wang et al., 2016). However, it is well known that prolonged exposure of estrogens plays a role in the breast cancer etiology, especially in postmenopausal women (Takemura et al., 2010). As in most other countries, breast cancer is now the most common cancer in Chinese women; cases in China account for 9.6% of all deaths from breast cancer worldwide (Fan et al., 2014). CYP1A1, 1B1, and 1A2 were demonstrated to mainly catalyze the oxidation of E2 to 2-OHE2 and 4-OHE2 (Lee et al., 2003). The 2-hydroxylation pathway negatively correlates with breast cancer risk, whereas the 4-hydroxylation pathway is likely an important initiator and promotor in breast cancer (Dunlap et al., 2017). 4-OHE2 is biotransformed to 3,4-E2-quinone, a known electrophilic species, causing the formation of DNA adducts and tumorigenesis (Yager, 2015; Wang et al., 2016). Reactive oxygen species can be also produced in this metabolic pathway, contributing to oxidative DNA damage. 2-Methoxyestradiol, generated from the metabolism of catechol by catechol-*O*-methyltransferase, blocks the further oxidation of 2-OHE2. Meanwhile, 2-methoxyestradiol, an inhibitor of CYP1B1, which is responsible for the 4-hydroxylation pathway, has been recently considered to be a promising agent to fight metastatic breast cancer (Schwarz et al., 2011). Thus, 2-OHE2 and 4-OHE2 may be regarded as detoxification and genotoxic biomarkers, respectively (Scheme 2). Our results showed that the formation of 2-OHE2 was primarily mediated by CYP1A1 and CYP1A2, and the formation of 4-OHE2 was primarily mediated by CYP1B1 (Scheme 2), which is consistent with a previous report (Itoh et al., 2010). The catalytic efficiency of E2 2-hydroxylation and 4-hydroxylation by CYP1A1 is approximately 255-fold higher than that of CYP1A2 (55-fold) and CYP1B1 (0.14-fold) (Table 3). Nevertheless, the IC_{50} value for NC-induced inhibition of E2 2-hydroxylation by CYP1A1 was about 60% of the value of 4-hydroxylation, indicating that NC is more potent in inhibiting the generation of 2-OHE2 (Table 3). Kinetic analysis displayed that NC is a mixed type of inhibitor of E2 2-hydroxylation with K_i and K_I values of 0.052 and 0.21 μM, and a competitive inhibitor of E2 4-hydroxylation with a K_i value of 0.26 μM (Fig. 6; Table 4). No significant inhibition of E2 metabolism induced by NC was observed in CYP1B1 or CYP1A2 incubation systems. Additionally, the MCF-7 cell model study showed that NC significantly decreased the formation of 2-OHE2 (Fig. 7). Given together, the effect of NC on E2 chemical carcinogenesis is proposed as shown in Scheme 2. These data suggest that the NC-induced inhibitory effect on E2 oxidative metabolism in vitro was mainly contributed by the CYP1A1-mediated 2-hydroxylation pathway. The reduced production of 2-methoxyestradiol may relatively result in the accumulation of 4-OHE2. Thus, potential drug-drug interactions should be considered in the dosage regimen of NC for chemoprotection against the toxicity of 4-OHE2.

In conclusion, NC is a mixed type of inhibitor of CYP1A1 and a competitive inhibitor of CYP1B1. The observed preferential inhibition of NC on CYP1A1-mediated E2 2-hydroxylation suggests that 4-OHE2-mediated genotoxicity might be increased by NC.

Authorship Contributions

Participated in research design: Mao, Zheng, Peng.
Conducted experiments: Mao, Q. Wang, Yang, Li, Lin.
Performed data analysis: Mao, J. Wang.
Wrote or contributed to the writing of the manuscript: Mao, Zheng.

References

Arthur HR, Hui WH, and Ng YL (1959) An examination of the rutaceae of Hong Kong. Part II. The alkaloids, nitidine and oxynitidine, from *Zanthoxylum nitidum*. *J Chem Soc* **0**:1840–1845.
Bouquet J, Rivaud M, Chevalley S, Deharo E, Jullian V, and Valentin A (2012) Biological activities of nitidine, a potential anti-malarial lead compound. *Malar J* **11**:67.
Chen J, Wang J, Lin L, He L, Wu Y, Zhang L, Yi Z, Chen Y, Pang X, and Liu M (2012) Inhibition of STAT3 signaling pathway by nitidine chloride suppressed the angiogenesis and growth of human gastric cancer. *Mol Cancer Ther* **11**:277–287.
Danton AC, Montastruc F, Sommet A, Durrieu G, Bagheri H, Bondon-Guitton E, Lapeyre-Mestre M, and Montastruc JL (2013) Importance of cytochrome P450 (CYP450) in adverse drug reactions due to drug-drug interactions: a PharmacoVigilance study in France. *Eur J Clin Pharmacol* **69**:885–888.
Dunlap TL, Howell CE, Mukand N, Chen SN, Pauli GF, Dietz BM, and Bolton JL (2017) Red clover aryl hydrocarbon receptor (AhR) and estrogen receptor (ER) agonists enhance genotoxic estrogen metabolism. *Chem Res Toxicol* **30**:2084–2092.
Fan L, Strasser-Weippl K, Li JJ, St Louis J, Finkelstein DM, Yu KD, Chen WQ, Shao ZM, and Goss PE (2014) Breast cancer in China. *Lancet Oncol* **15**:e279–e289.
Fang Z, Tang Y, Jiao W, Xing Z, Guo Z, Wang W, Xu Z, and Liu Z (2014) Nitidine chloride induces apoptosis and inhibits tumor cell proliferation via suppressing ERK signaling pathway in renal cancer. *Food Chem Toxicol* **66**:210–216.
Foti RS and Dalvie DK (2016) Cytochrome P450 and non-cytochrome P450 oxidative metabolism: contributions to the pharmacokinetics, safety, and efficacy of xenobiotics [Published correction appears in Drug Metab Dispos (2016) 44:1516]. *Drug Metab Dispos* **44**:1229–1245.
Gakunju DM, Mberu EK, Dossaji SF, Gray AI, Waigh RD, Waterman PG, and Watkins WM (1995) Potent antimalarial activity of the alkaloid nitidine, isolated from a Kenyan herbal remedy. *Antimicrob Agents Chemother* **39**:2606–2609.
Henderson MC, Miranda CL, Stevens JF, Deinzer ML, and Buhler DR (2000) In vitro inhibition of human P450 enzymes by prenylated flavonoids from hops, *Humulus lupulus*. *Xenobiotica* **30**: 235–251.
Hu J, Zhang WD, Liu RH, Zhang C, Shen YH, Li HL, Liang MJ, and Xu XK (2006) Benzophenanthridine alkaloids from *Zanthoxylum nitidum* (Roxb.) DC, and their analgesic and anti-inflammatory activities. *Chem Biodivers* **3**:990–995.
Itoh T, Takemura H, Shimoi K, and Yamamoto K (2010) A 3D model of CYP1B1 explains the dominant 4-hydroxylation of estradiol. *J Chem Inf Model* **50**:1173–1178.
Iwasaki H, Okabe T, Takara K, Toda T, Shimatani M, and Oku H (2010) Tumor-selective cytotoxicity of benzo[c]phenanthridine derivatives from *Toddalia asiatica* Lam. *Cancer Chemother Pharmacol* **65**:719–726.
Lakhani NJ, Sarkar MA, Venitz J, and Figg WD (2003) 2-Methoxyestradiol, a promising anticancer agent. *Pharmacotherapy* **23**:165–172.
Lee AJ, Cai MX, Thomas PE, Conney AH, and Zhu BT (2003) Characterization of the oxidative metabolites of 17β-estradiol and estrone formed by 15 selectively expressed human cytochrome P450 isoforms. *Endocrinology* **144**:3382–3398.
Lee D, Perez P, Jackson W, Chin T, Galbreath M, Fronczek FR, Isovitsch R, and Iimoto DS (2016) Aryl morpholino triazenes inhibit cytochrome P450 1A1 and 1B1. *Bioorg Med Chem Lett* **26**: 3243–3247.

Downloaded from dmd.aspetjournals.org at ASPET Journals on April 16, 2024

Li W, Yin H, Bardelang D, Xiao J, Zheng Y, and Wang R (2017) Supramolecular formulation of nitidine chloride can alleviate its hepatotoxicity and improve its anticancer activity. *Food Chem Toxicol* **109**:923–929.

Liao J, Xu T, Zheng JX, Lin JM, Cai QY, Yu DB, and Peng J (2013) Nitidine chloride inhibits hepatocellular carcinoma cell growth in vivo through the suppression of the JAK1/STAT3 signaling pathway. *Int J Mol Med* **32**:79–84.

Liu L, Sun S, Rui H, and Li X (2017) In vitro inhibitory effects of dihydromyricetin on human liver cytochrome P450 enzymes. *Pharm Biol* **55**:1868–1874.

Lo SN, Chang YP, Tsai KC, Chang CY, Wu TS, and Ueng YF (2013) Inhibition of CYP1 by berberine, palmatine, and jatrorrhizine: selectivity, kinetic characterization, and molecular modeling. *Toxicol Appl Pharmacol* **272**:671–680.

Lo SN, Shen CC, Chang CY, Tsai KC, Huang CC, Wu TS, and Ueng YF (2015) The effect of oxidation on berberine-mediated CYP1 inhibition: oxidation behavior and metabolite-mediated inhibition. *Drug Metab Dispos* **43**:1100–1107.

Lozan E, Shinkaruk S, Al Abed SA, Lamothe V, Potier M, Marighetto A, Schmitter JM, Bennetau-Pelissero C, and Buré C (2017) Derivatization-free LC-MS/MS method for estrogen quantification in mouse brain highlights a local metabolic regulation after oral versus subcutaneous administration. *Anal Bioanal Chem* **409**:5279–5289.

Mao X, Hu Z, Wang Q, Zhang N, Zhou S, Peng Y, and Zheng J (2018) Nitidine chloride is a mechanism-based inactivator of CYP2D6. *Drug Metab Dispos* **46**:1137–1145.

Ou X, Lu Y, Liao L, Li D, Liu L, Liu H, and Xu H (2015) Nitidine chloride induces apoptosis in human hepatocellular carcinoma cells through a pathway involving p53, p21, Bax and Bcl-2. *Oncol Rep* **33**:1264–1274.

Pan X, Han H, Wang L, Yang L, Li R, Li Z, Liu J, Zhao Q, Qian M, Liu M, et al. (2011) Nitidine chloride inhibits breast cancer cells migration and invasion by suppressing c-Src/FAK associated signaling pathway. *Cancer Lett* **313**:181–191.

Schwarz D, Kisselev P, Schunck WH, and Roots I (2011) Inhibition of 17β-estradiol activation by CYP1A1: genotype- and regioselective inhibition by St. John's Wort and several natural polyphenols. *Biochim Biophys Acta* **1814**:168–174.

Shimada T (2017) Inhibition of carcinogen-activating cytochrome P450 enzymes by xenobiotic chemicals in relation to antimutagenicity and anticarcinogenicity. *Toxicol Res* **33**:79–96.

Takemura H, Uchiyama H, Ohura T, Sakakibara H, Kuruto R, Amagai T, and Shimoi K (2010) A methoxyflavonoid, chrysoeriol, selectively inhibits the formation of a carcinogenic estrogen metabolite in MCF-7 breast cancer cells. *J Steroid Biochem Mol Biol* **118**:70–76.

Tan GT, Pezzuto JM, Kinghorn AD, and Hughes SH (1991) Evaluation of natural products as inhibitors of human immunodeficiency virus type 1 (HIV-1) reverse transcriptase. *J Nat Prod* **54**:143–154.

VandenBrink BM and Isoherranen N (2010) The role of metabolites in predicting drug-drug interactions: focus on irreversible cytochrome P450 inhibition. *Curr Opin Drug Discov Devel* **13**:66–77.

Vrba J, Kosina P, Ulrichová J, and Modrianský M (2004) Involvement of cytochrome P450 1A in sanguinarine detoxication. *Toxicol Lett* **151**:375–387.

Wang S, Dunlap TL, Howell CE, Mbachu OC, Rue EA, Phansalkar R, Chen SN, Pauli GF, Dietz BM, and Bolton JL (2016) Hop (*Humulus lupulus* L.) extract and 6-prenylnaringenin induce P450 1A1 catalyzed estrogen 2-hydroxylation. *Chem Res Toxicol* **29**:1142–1150.

Wang Z, Jiang W, Zhang Z, Qian M, and Du B (2012) Nitidine chloride inhibits LPS-induced inflammatory cytokines production via MAPK and NF-kappaB pathway in RAW 264.7 cells. *J Ethnopharmacol* **144**:145–150.

Yager JD (2015) Mechanisms of estrogen carcinogenesis: the role of E2/E1-quinone metabolites suggests new approaches to preventive intervention—A review. *Steroids* **99**:56–60.

Zanger UM and Schwab M (2013) Cytochrome P450 enzymes in drug metabolism: regulation of gene expression, enzyme activities, and impact of genetic variation. *Pharmacol Ther* **138**:103–141.

Address correspondence to: Dr. Jiang Zheng, Wuya College of Innovation, Shenyang Pharmaceutical University, Shenyang, P. R., China; [b]State Key Laboratory of Functions and Applications of Medicinal Plants, Key Laboratory of Pharmaceutics of Guizhou Province, Guizhou Medical University, Guiyang, Guizhou, 550004, P. R. China. E-mail: zhengneu@yahoo.com; or Dr. Ying Peng, Wuya College of Innovation, Shenyang Pharmaceutical University, Shenyang, Liaoning, 110016, P. R. China. E-mail: yingpeng1999@163.com

Downloaded from dmd.aspetjournals.org at ASPET Journals on April 16, 2024